Uplink Achievable Rate analysis of Massive MIMO Systems in Transmit-correlated Ricean Fading Environments

Yixin Xu[1*], Fulai Liu [2,1*], Zixuan Zhang[2], Zhenxing Sun[1]
[1] School of Computer Science and Engineering, Northeastern University, Shenyang, China
[e-mail: xuyixin510@126.com , sunzx-0@163.com]
[2] Engineer Optimization & Smart Antenna Institute, Northeastern University at Qinhuangdao, Qinhuangdao, China
[e-mail: fulailiu@126.com, zhangzx339@126.com]
[*]Corresponding author: Yixin Xu and Fulai Liu

Received November 10, 2022; revised January 6, 2023; accepted January 23, 2023; published January 31, 2023

Abstract

In this article, the uplink achievable rate is investigated for massive multiple-input multiple-output (MIMO) under correlated Ricean fading channel, where each base station (BS) and user are both deployed multiple antennas. Considering the availability of prior knowledge at BS, two different channel estimation approaches are adopted with and without prior knowledge. Based on these channel estimations, a two-layer decoding scheme is adopted with maximum ratio precoding as the first layer decoder and optimal second layer precoding in the second layer. Based on two aforementioned channel estimations and two-layer decoding scheme, the exact closed form expressions for uplink achievable rates are computed with and without prior knowledge, respectively. These derived expressions enable us to analyze the impacts of line-of-sight (LoS) component, two-layer decoding, data transmit power, pilot contamination, and spatially correlated Ricean fading. Then, numerical results illustrate that the system with spatially correlated Ricean fading channel is superior in terms of uplink achievable rate. Besides, it reveals that compared with the single-layer decoding, the two-layer decoding scheme can significantly improve the uplink achievable rate performance.

Keywords: Ricean fading, massive MIMO, spatially correlated channel, multi-antenna users, two-layer decoding.

This work was supported by the National Nature Science Foundation of China under Grant No.61971117 and by the Natural Science Foundation of Hebei Province (Grant No. F2020501007).

http://doi.org/10.3837/tiis.2023.01.014 **ISSN : 1976-7277**

1. Introduction

Massive multiple-input multiple-output (MIMO) is an important technique for beyond-5G (B5G) communication networks, since its ability to enhance system performance (e.g. spectral and energy efficiency) with large antenna arrays [1]. In practice, most of the studies mainly focus on analyzing massive MIMO performance for single-antenna user scenario, e.g. [2-4]. On this basis, the system performance will be significantly improved by using deep learning which has many advantages in massive training samples, noise influence, and high-dimensional feature data [5, 6]. However, many modern user devices such as smart vehicles, tablets, and laptops are equipped with multi-antennas to enhance the achievable rate performance [7, 8]. Thus, as one of performance metrics for massive MIMO, the achievable rate of multi-antenna users is necessary to be analyzed for understanding the effects of additional antennas at users [9, 10].

To this end, for a single-cell scenario with multi-antenna users, both uplink and downlink achievable rates are derived under spatially correlated Rayleigh fading channel [11]. It shows that the additional user antennas can significantly improve the achievable rate via increasing spatial multiplexing. However, a novel insight is presented in [12], which reveals that the inner-user interference seriously affects the achievable rate when the users are deployed multiple antennas. For mitigating interference, a hybrid beamformer is proposed by using the channel covariance matrix [13]. Moreover, an improved maximum ratio (MR) precoding scheme is presented for multi-antenna users to mitigate the interference in [14, 15]. Compared with the conventional precoder, this precoder can significantly enhance the downlink achievable rate. In a multi-cell scenario, employing zero forcing (ZF) and regularized ZF (RZF) precoding scheme, the closed-form downlink achievable rates are derived [16]. It validates that the achievable rates are significantly affected by pilot contamination (PC). Based on the interference alignment theory, a novel approach is presented to reduce PC via designing precoder and combiner matrices [17]. In addition, combining the benefits of the spatial modulation and massive MIMO techniques, the closed form achievable rate expressions are derived with the MR and ZF combining precoders, respectively [18]. This expression facilitated the system-level analysis, in which the system-level achievable rates are maximized by optimizing the user antennas.

The aforementioned research focuses on investigating the system performance under Rayleigh fading channel. However, the practical channel in densely deployed massive MIMO system is always composed of line-of-sight (LoS) components, which should be modeled as spatially correlated Ricean fading [19]. To this end, for a single-cell scenario with multi-antenna users, the closed-form uplink achievable rate expression is computed under correlated Ricean fading in [20]. However, this study assumes that the full knowledge of channel covariance matrices is known at the BS as prior information, while practical BS sometimes does not obtain any prior information. Moreover, the impact of PC is not considered in this study. In fact, PC is still challenging and cannot be ignored [21]. To mitigate PC, a two-layer decoding scheme is studied for massive MIMO with single-antenna users in [22]. However, this work focuses on the system with single-antenna users, and only considers the case that the full knowledge of channel covariance matrices is known at the BS.

Motivated by the aforementioned observations, the uplink achievable rate for multi-cell scenario with multi-antenna users is investigated in this article under correlated Ricean fading channel by capturing the effects of LoS components, PC, two-layer decoding, and data

transmit power. The specific contributions of this article are outlined as follows:

(1) A multi-cell multi-antenna users massive MIMO network is proposed under spatially correlated Ricean fading that captures the effect of LoS and non-line-of-sight (NLoS) components in real communication systems. Particularly, the Kronecker correlation channel model is adopted for describing LoS propagation and spatially correlated multipath fading.

(2) By employing two different channel estimations and two-layer decoding scheme, the closed-form achievable rate expressions are computed under correlated Ricean fading channel. These derived expressions provide generalized expression for analyzing the impacts of multi-antenna users, inter-cell interference, channel estimation errors and spatially correlated Ricean fading. Simulation results illustrate that the uplink achievable rate is significantly improved by employing two-layer decoding scheme under correlated Ricean fading channel.

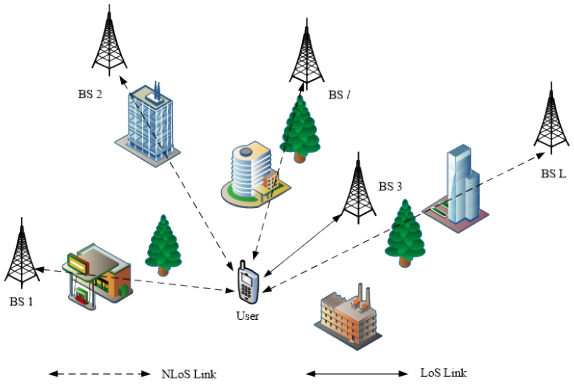

Fig. 1. Illustration for massive MIMO network under Ricean fading.

2. System Model

In this work, an uplink massive MIMO network with L cells is consider, where each cell contains that one BS simultaneously serves K users. In particular, each user and BS are deployed with N and M antennas, respectively. For the sake of brevity, the sets of BS, users, and user antenna are denoted as $\mathcal{L} \in \{1,...,L\}$, $\mathcal{K} \in \{1,...,K\}$, and $\mathcal{N} \in \{1,...,N\}$, respectively. Moreover, the kth user in the ith cell is defined as $\mathbf{u}_{ik}$, where $k \in \mathcal{K}$ and $i \in \mathcal{L}$. The channel matrix between $\mathbf{u}_{ik}$ and the lth BS is defined as $\boldsymbol{H}_{ik}^{l} = \left[\boldsymbol{h}_{ik}^{l1},...,\boldsymbol{h}_{ik}^{lN}\right] \in \mathbb{C}^{M \times N}$, where $\boldsymbol{h}_{ik}^{ln} \in \mathbb{C}^{M \times 1}$ represents the channel vector between nth antenna of $\mathbf{u}_{ik}$ and the lth BS. Furthermore, the length of coherence interval is denoted by τ_c. Each coherence interval consists of two parts: τ_p ($\tau_p \geq KN$) and $\tau_c - \tau_p$ symbols are utilized for uplink training and data transmission, respectively.

In practical scenario, the LoS path can be obstructed due to the presence of blockages as shown in **Fig. 1**. Thus, the channel is needed to be characterized as a combination of both LoS and NLoS components. For this purpose, based on Kronecker correlation model [23], the Ricean fading channel $\boldsymbol{H}_{ik}^{l}$ is given by

$$\boldsymbol{H}_{ik}^{l} = \bar{\boldsymbol{H}}_{ik}^{l} + \underbrace{(\boldsymbol{R}_{ik}^{l})^{1/2} \boldsymbol{G}_{ik}^{l} (\boldsymbol{U}_{ik}^{l})^{1/2}}_{\tilde{\boldsymbol{G}}_{ik}^{l}} \tag{1}$$

where $\bar{\boldsymbol{H}}_{ik}^{l}=\left[\bar{\boldsymbol{h}}_{ik}^{l1},...,\bar{\boldsymbol{h}}_{ik}^{lN}\right]\in\mathbb{C}^{M\times N}$ is an matrix corresponds to the deterministic LoS component and $\tilde{\boldsymbol{G}}_{ik}^{l}=\left[\tilde{\boldsymbol{g}}_{ik}^{l1},...,\tilde{\boldsymbol{g}}_{ik}^{lN}\right]\in\mathbb{C}^{M\times N}$ represents the stochastic NLoS component. In (1), $\boldsymbol{R}_{ik}^{l}\in\mathbb{C}^{M\times M}$ stands for a covariance matrix at lth BS. $\boldsymbol{G}_{ik}^{l}$ represents the $M\times N$ small-scale fading matrix, and the elements of $\boldsymbol{G}_{ik}^{l}$ obey distribution with $C\mathcal{N}(0,1)$. Moreover, $\boldsymbol{U}_{ik}^{l}\in\mathbb{C}^{N\times N}$ is a covariance matrix capturing the spatial correlation at u_{ik}. Let $\boldsymbol{U}_{ik}^{l}=\tilde{\boldsymbol{U}}_{ik}^{l}\boldsymbol{\Lambda}_{ik}^{l}\tilde{\boldsymbol{U}}_{ik}^{l}$ be the eigenvalue decomposition of $\boldsymbol{U}_{ik}^{l}$, where $\tilde{\boldsymbol{U}}_{ik}^{l}\in\mathbb{C}^{N\times N}$ is a unitary matrix and $\boldsymbol{\Lambda}_{ik}^{l}=\mathrm{diag}\left\{\lambda_{ik}^{l1},\cdots\lambda_{ik}^{lN}\right\}$ contains the eigenvalues of $\boldsymbol{U}_{ik}^{l}$.

2.1 Uplink Pilot Training

In pilot-based channel estimation phase, all users are required to simultaneously send pilot sequences to the BS for channel estimation. Let $\boldsymbol{\Phi}_{lk}=\left[\boldsymbol{\phi}_{lk,1}^{l},...,\boldsymbol{\phi}_{lk,N}^{l}\right]\in\mathbb{C}^{\tau_p\times N}$ be the pilot sequence matrix of u_{lk}, satisfying that

$$\boldsymbol{\Phi}_{lk}^{\mathrm{H}}\boldsymbol{\Phi}_{l'k'}=\begin{cases}\tau_p\boldsymbol{I}_N & k=k',\\ \boldsymbol{0}_{N\times N} & k\neq k'.\end{cases}\tag{2}$$

The pilot signals $\boldsymbol{Y}_{l}^{p}\in\mathbb{C}^{M\times\tau_p}$ received at lth BS is expressed as

$$\boldsymbol{Y}_{l}^{p}=\sum_{l\in\mathcal{L}}\sum_{k\in\mathcal{K}}\sqrt{\rho_u}\boldsymbol{H}_{lk}^{l}(\boldsymbol{\Phi}_{lk})^{\mathrm{H}}+\boldsymbol{N}_{l},\tag{3}$$

where ρ_u represents the transmitted pilot power. $\boldsymbol{N}_{l}\in\mathbb{C}^{M\times\tau_p}$ denotes the additive noise matrix, and the elements of $\boldsymbol{N}_{l}$ obey distribution with $C\mathcal{N}(0,1)$.

To obtain the channel estimation of $\boldsymbol{h}_{lk}^{l}$, $\boldsymbol{Y}_{l}^{p}$ is projecting onto $\boldsymbol{\Phi}_{lk}$ as follows:

$$\boldsymbol{Y}_{lk}^{p}=\boldsymbol{Y}_{l}^{p}\boldsymbol{\Phi}_{lk}=\sqrt{\rho_u}\tau_p\boldsymbol{H}_{lk}^{l}+\sum_{l'\neq l}\sqrt{\rho_u}\tau_p\boldsymbol{H}_{l'k}^{l}+\boldsymbol{N}_{l}\boldsymbol{\Phi}_{lk}.\tag{4}$$

Let $\hat{\boldsymbol{H}}_{lk}^{l,\mathrm{MMSE}}=\left[\hat{\boldsymbol{h}}_{lk}^{l1,\mathrm{MMSE}},...,\hat{\boldsymbol{h}}_{lk}^{lN,\mathrm{MMSE}}\right]\in\mathbb{C}^{M\times N}$ denote the minimum mean-squared error (MMSE) estimation of $\boldsymbol{H}_{lk}^{l}$, which is expressed as [24]

$$\mathrm{vec}(\hat{\boldsymbol{H}}_{lk}^{l,\mathrm{MMSE}})=\mathrm{vec}(\bar{\boldsymbol{H}}_{lk}^{l})+(\boldsymbol{\Lambda}_{lk}^{l}\otimes\boldsymbol{R}_{lk}^{l})(\sum_{l'=1}^{L}\boldsymbol{\Lambda}_{l'k}^{l}\otimes\boldsymbol{R}_{l'k}^{l}+(\tau_p\sqrt{\rho_u})^{-1}\boldsymbol{I}_N\otimes\boldsymbol{I}_M)^{-1}\mathrm{vec}(\boldsymbol{Y}_{lk}^{p}-\tilde{\boldsymbol{Y}}_{lk}^{p}),\tag{5}$$

where $\tilde{\boldsymbol{Y}}_{lk}^{p}=\sum_{l'\in\mathcal{L}}\tau_p\sqrt{\rho_u}\bar{\boldsymbol{H}}_{l'k}^{l}$.

Moreover, let $\bar{\boldsymbol{h}}_{lk}^{ln}$ and $\tilde{\boldsymbol{g}}_{lk}^{ln}$ be nth column of $\bar{\boldsymbol{H}}_{lk}^{l}$ and $\tilde{\boldsymbol{G}}_{lk}^{l}$, respectively. Then, the MMSE estimation in (5) is represented as

$$\begin{bmatrix}\hat{\boldsymbol{h}}_{lk}^{l1,\mathrm{MMSE}}\\ \vdots\\ \hat{\boldsymbol{h}}_{lk}^{lN,\mathrm{MMSE}}\end{bmatrix}^{\mathrm{T}}=\begin{bmatrix}\bar{\boldsymbol{h}}_{lk}^{l1}\\ \vdots\\ \bar{\boldsymbol{h}}_{lk}^{lN}\end{bmatrix}^{\mathrm{T}}+\boldsymbol{\Xi}\begin{bmatrix}\sum_{l'\in\mathcal{L}}\tau_p\sqrt{\rho_u}\tilde{\boldsymbol{g}}_{l'k}^{l1}+\boldsymbol{n}_{lk}\\ \vdots\\ \sum_{l'\in\mathcal{L}}\tau_p\sqrt{\rho_u}\tilde{\boldsymbol{g}}_{l'k}^{lN}+\boldsymbol{n}_{lk}\end{bmatrix}^{\mathrm{T}},\tag{6}$$

where $\boldsymbol{\Xi}=\mathrm{diag}\left\{\lambda_{lk,}^{l1}\boldsymbol{R}_{lk}^{l}(\boldsymbol{Q}_{lk}^{1})^{-1},\cdots,\lambda_{lk}^{lN}\boldsymbol{R}_{lk}^{l}(\boldsymbol{Q}_{lk}^{N})^{-1}\right\}$ and $\boldsymbol{n}_{lk}=\mathrm{vec}(\boldsymbol{N}_{l}\boldsymbol{\Phi}_{lk})$. Here, $\boldsymbol{Q}_{lk}^{n}=\sum_{l'\in\mathcal{L}}\lambda_{l'k}^{ln}\boldsymbol{R}_{l'k}^{l}+(\tau_p\rho_u)^{-1}\boldsymbol{I}_M$.

Based on (6), the MMSE estimation $\hat{\boldsymbol{h}}_{lk}^{ln,\mathrm{MMSE}}$ and the estimation error $\tilde{\boldsymbol{h}}_{lk}^{ln,\mathrm{MMSE}} = \boldsymbol{h}_{lk}^{ln} - \hat{\boldsymbol{h}}_{lk}^{ln,\mathrm{MMSE}}$ are distributed as

$$\hat{\boldsymbol{h}}_{lk}^{ln,\mathrm{MMSE}} \sim \mathcal{CN}\left(\bar{\boldsymbol{h}}_{lk}^{ln}, \boldsymbol{\Omega}_{lk}^{ln}\right), \tag{7}$$

$$\tilde{\boldsymbol{h}}_{lk}^{ln,\mathrm{MMSE}} \sim \mathcal{CN}\left(0, \boldsymbol{C}_{lk}^{ln}\right), \tag{8}$$

where $\boldsymbol{\Omega}_{lk}^{ln} = (\lambda_{lk}^{ln})^2 \boldsymbol{R}_{lk}^{l} (\boldsymbol{Q}_{lk}^{n})^{-1} \boldsymbol{R}_{lk}^{l}$ and $\boldsymbol{C}_{lk}^{ln} = \lambda_{lk}^{ln} \boldsymbol{R}_{lk}^{l} - \boldsymbol{\Omega}_{lk}^{l}$.

Note that the full knowledge of covariance matrices $\boldsymbol{R}_{lk}^{l}$ is required for MMSE channel estimation as prior information. For another practical scenario, if there is no prior information of $\boldsymbol{R}_{lk}^{l}$, we can use the least-square (LS) approach to achieve the estimation of $\hat{\boldsymbol{h}}_{lk,n}^{l}$ [25]. Based on this method, the LS estimation $\hat{\boldsymbol{h}}_{lk}^{ln}$ is given by $\hat{\boldsymbol{h}}_{lk}^{ln,\mathrm{LS}} = (1/\tau_p\sqrt{\rho_u})\,\hat{\boldsymbol{y}}_{lk,n}$, where $\hat{\boldsymbol{y}}_{lk,n} = \sum_{l' \in \mathcal{L}} \boldsymbol{h}_{l'k}^{ln} + \boldsymbol{n}_{l'k}$ denotes the nth column of $\boldsymbol{Y}_{lk}^{p}$. Moreover, the LS estimation $\hat{\boldsymbol{h}}_{lk}^{ln}$ and estimation error $\tilde{\boldsymbol{h}}_{lk}^{ln}$ can be distributed as

$$\hat{\boldsymbol{h}}_{lk}^{ln,\mathrm{LS}} \sim \mathcal{CN}\left(\frac{1}{\tau_p\sqrt{\rho_u}}\bar{\boldsymbol{y}}_{lk,n}, \frac{1}{\tau_p\rho_u}\boldsymbol{Q}_{lk}^{ln}\right), \tag{9}$$

$$\tilde{\boldsymbol{h}}_{lk}^{ln,\mathrm{LS}} \sim \mathcal{CN}\left(\bar{\boldsymbol{h}}_{lk}^{ln} - \frac{1}{\tau_p\sqrt{\rho_u}}\bar{\boldsymbol{y}}_{lk,n}, \frac{1}{\tau_p\rho_u}\boldsymbol{Q}_{lk}^{ln} - \lambda_{lk}^{ln}\boldsymbol{R}_{lk}^{l}\right), \tag{10}$$

where $\bar{\boldsymbol{y}}_{lk,n} = \sum_{l' \in \mathcal{L}} \tau_p \sqrt{\rho_u} \bar{\boldsymbol{h}}_{l'k}^{ln}$.

It is clear that the LS channel estimation is more complicated than the MMSE channel estimation. Specifically, the estimation error $\tilde{\boldsymbol{h}}_{lk}^{ln}$ has non-zero mean, which is required to be considered for analyzing the system performance.

2.2 Uplink Data Transmission

The received data signal $\boldsymbol{y}_l \in \mathbb{C}^{M\times 1}$ at the lth BS is given by

$$\boldsymbol{y}_l = \sum_{l'' \in \mathcal{L}} \sum_{i \in \mathcal{C}} \boldsymbol{H}_{l''i}^{l} \boldsymbol{F}_{l''i} \boldsymbol{x}_{l''i} + \tilde{\boldsymbol{n}}_l. \tag{11}$$

where $\boldsymbol{x}_{l''i} = [x_{l''i}^{1}, ..., x_{l''i}^{N}]^{\mathrm{T}} \in \mathbb{C}^{N\times 1}$ is the uplink data signal transmitted from $\mathrm{u}_{l''i}$ to the BS, satisfying $\mathbb{E}\left\{\boldsymbol{x}_{l''i}(\boldsymbol{x}_{l''i})^{\mathrm{H}}\right\} = \boldsymbol{I}_N$. Moreover, $\boldsymbol{F}_{l''i} = \mathrm{diag}[p_{l''i}^{1}, ..., p_{l''i}^{N}] \in \mathbb{C}^{N\times N}$ denotes the uplink transmit power of $\mathrm{u}_{l''i}$ and $\tilde{\boldsymbol{n}}_l \in \mathbb{C}^{M\times 1}$ represents the additive noise at lth BS, satisfying $\mathbb{E}\left\{\tilde{\boldsymbol{n}}_l(\tilde{\boldsymbol{n}}_l)^{\mathrm{H}}\right\} = \boldsymbol{I}_M$.

3. Uplink Achievable Rate Analysis

The exact closed form expressions in terms of uplink achievable rate are computed in this section by employing two-layer decoding scheme based on MMSE and LS channel estimation, respectively. Particularly, the main idea of two-layer decoding scheme is that the received data signal is first decoded by local decoding (i.e. MR precoding) at the BS to suppress intra-cell interference. Then, the decoded signals of users that shared the same pilot are collected by a central station for jointly processing in the second layer to mitigate PC and inter-cell interference.

3.1 Uplink Achievable Rate

Let $\boldsymbol{W}_{lk} = [\boldsymbol{w}_{lk}^1, ..., \boldsymbol{w}_{lk}^N] \in \mathbb{C}^{M \times N}$ denote the MR combining matrix in the first layer, of which the nth column is defined as $\boldsymbol{w}_{lk}^n = \hat{\boldsymbol{h}}_{lk}^{ln}$. Then, the local estimate of $\boldsymbol{y}_l$ is written as $\boldsymbol{s}_{lk} = (\boldsymbol{W}_{lk})^{\mathrm{H}} \boldsymbol{y}_l$.

Extracting the nth row of $\boldsymbol{s}_{lk}$, the nth data-stream received at the BS is given by

$$\boldsymbol{s}_{lk}^n = \underbrace{p_{lk}^n (\boldsymbol{w}_{lk}^n)^{\mathrm{H}} \boldsymbol{h}_{lk}^n x_{lk}^n}_{\text{Desired signal}} + \underbrace{\sum_{m \in \mathcal{N} \setminus \{n\}} p_{lk}^m (\boldsymbol{w}_{lk}^n)^{\mathrm{H}} \boldsymbol{h}_{lk}^{lm} x_{lk}^m}_{\text{Inner-user interference}} + \underbrace{\sum_{l'' \in \mathcal{L} \setminus \{l\}} \sum_{k' \in \mathcal{K}} \sum_{m \in \mathcal{N}} p_{l''k'}^m (\boldsymbol{w}_{lk}^n)^{\mathrm{H}} \boldsymbol{h}_{l''k'}^{lm} x_{l''k'}^m}_{\text{Inter-cell interference}}$$

$$+ \underbrace{\sum_{k' \in \mathcal{K} \setminus \{k\}} \sum_{m \in \mathcal{N}} p_{lk'}^m (\boldsymbol{w}_{lk}^n)^{\mathrm{H}} \boldsymbol{h}_{lk'}^{lm} x_{lk'}^m}_{\text{Intra-cell interference}} + \underbrace{(\boldsymbol{w}_{lk}^n)^{\mathrm{H}} \overline{\boldsymbol{n}}_l}_{\text{Noise}} \tag{12}$$

where $\overline{\boldsymbol{n}}_l \sim C\mathcal{N}(0,1)$ denotes the additive noise component.

After that, the first-layer decoding signals in (12) are converged to a central station for the second-layer decoding as

$$\hat{\boldsymbol{s}}_{lk}^n = \sum_{l' \in \mathcal{L}} (a_{lk,n}^{l'})^{\mathrm{H}} \boldsymbol{s}_{l'k}^n \tag{13}$$

where $a_{lk,n}^{l'}$ is the second-layer decoding weight.

Define that $\boldsymbol{b}_{lkk',nm} = \left[(\boldsymbol{w}_{1k}^n)^{\mathrm{H}} \boldsymbol{h}_{lk'}^{1m}, ..., (\boldsymbol{w}_{Lk}^n)^{\mathrm{H}} \boldsymbol{h}_{lk'}^{Lm} \right]^{\mathrm{T}} \in \mathbb{C}^L$ and $\mathbf{a}_{lk}^n = \left[a_{lk,n}^1, ..., a_{lk,n}^L \right]^{\mathrm{T}} \in \mathbb{C}^L$, then the signal $\hat{\boldsymbol{s}}_{lk}^n$ is represented by

$$\hat{\boldsymbol{s}}_{lk}^n = p_{lk}^n (\mathbf{a}_{lk}^n)^{\mathrm{H}} \boldsymbol{b}_{lkk,nn} x_{lk}^n + \sum_{m \in \mathcal{N} \setminus \{n\}} p_{lk}^m (\mathbf{a}_{lk}^n)^{\mathrm{H}} \boldsymbol{b}_{lkk,nm} x_{lk}^m + \sum_{k' \in \mathcal{K} \setminus \{k\}} \sum_{m \in \mathcal{N}} p_{lk'}^m (\mathbf{a}_{lk}^n)^{\mathrm{H}} \boldsymbol{b}_{lkk',nm} x_{lk'}^m + \hat{n}_{lk}$$

$$+ \sum_{l'' \in \mathcal{L} \setminus \{l\}} \sum_{k' \in \mathcal{K}} \sum_{m \in \mathcal{N}} p_{l''k'}^m (\mathbf{a}_{lk}^n)^{\mathrm{H}} \boldsymbol{b}_{l''kk',nm} x_{l''k'}^m . \tag{14}$$

where $\hat{n}_{lk} = \sum_{l' \in \mathcal{L}} (a_{lk,n}^{l'})^{\mathrm{H}} (\boldsymbol{w}_{lk}^n)^{\mathrm{H}} \overline{\boldsymbol{n}}_l$.

Based on (14), employing the use-and-then-forget (UatF) technique [26], the uplink achievable rate of u_{lk} with two-layer decoding scheme is given by

$$\tilde{\mathcal{R}}_{lk} = (1 - \frac{\tau_p}{\tau_c}) \sum_{n \in \mathcal{N}} \log_2 (1 + \gamma_{lk,n}), \tag{15}$$

where $\gamma_{lk,n}$ denotes signal to interference plus noise ratio (SINR) for the nth data-stream of u_{lk}, which is given by

$$\gamma_{lk,n} = \frac{\left| p_{lk}^n (\mathbf{a}_{lk}^n)^{\mathrm{H}} \mathbb{E}\{\boldsymbol{b}_{lkk,nn}\} \right|^2}{(\mathbf{a}_{lk}^n)^{\mathrm{H}} (\boldsymbol{D}_{lk}) \mathbf{a}_{lk}^n}, \tag{16}$$

where $\boldsymbol{D}_{lk} = \sum_{l'' \in \mathcal{L}} \sum_{k' \in \mathcal{K}} \sum_{m \in \mathcal{N}} (p_{l''k'}^m)^2 \boldsymbol{\Gamma}_{l''kk'} - (p_{lk}^n)^2 \mathbb{E}\{\boldsymbol{b}_{lkk,nn}\} \mathbb{E}\{(\boldsymbol{b}_{lkk,nn})^{\mathrm{H}}\} + \boldsymbol{Z}_{kn}$. Here, $\boldsymbol{Z}_{kn} = \mathrm{diag}(\mathbb{E}\{\|\boldsymbol{w}_{1k}^n\|^2\}, ..., \mathbb{E}\{\|\boldsymbol{w}_{Lk}^n\|^2\})$ and $\boldsymbol{\Gamma}_{l''kk'} = \mathbb{E}\{\boldsymbol{b}_{lkk,nm} (\boldsymbol{b}_{lkk,nm})^{\mathrm{H}}\} \in \mathbb{C}^{L \times L}$.

The expression (15) provides a generalized uplink achievable rate expression for a multi-cell scenario with multi-antenna users. Note that the expression (15) can be applied to practical spatially correlated Ricean fading channel with arbitrary channel estimation and first-layer decoder. However, the expression in (15) is not in closed-form, which cannot

effectively quantify the effects of LoS component, PC, and channel estimation error. Moreover, for enhancing the performance of system, the closed-form expressions are desired to formulate the optimization scheme such as data power control and resource allocation. To this end, using the MR combining as the first-layer decoder, the closed-form expressions of (15) are derived with and without prior knowledge in the next subsection.

In addition, it can be observed that the second-layer decoding vector $\mathbf{a}_{lk,n}$ seriously affects the performance expression. Thus, to enhance system performance, the second-layer decoding vector $\mathbf{a}_{lk,n}$ can be optimized by the following corollary.

Corollary 1: *For a given set of first-layer decoder (i.e. MR precoding) and data transmit power matrix, the uplink achievable rate in (15) can be maximized by*

$$\mathbf{a}_{lk}^{n*} = (\boldsymbol{D}_k)^{-1}\mathbb{E}\left\{\boldsymbol{b}_{lkk,nn}\right\} \tag{17}$$

and the maximum value of $\tilde{\mathcal{R}}_{lk}$ *can be given by*

$$\tilde{\mathcal{R}}_{lk}^{*} = (1-\frac{\tau_p}{\tau_c})\sum_{n\in\mathcal{N}}\log_2(1+(\mathbb{E}\left\{\boldsymbol{b}_{lkk,nn}\right\})^{\mathrm{H}}\left(\boldsymbol{D}_k\right)^{-1}\mathbb{E}\left\{\boldsymbol{b}_{lkk,nn}\right\}). \tag{18}$$

Proof: The SINR expression $\gamma_{lk,n}$ in (16) can be recognized as a generalized Rayleigh quotient with respect to $\mathbf{a}_{lk}^{n}$. Thus, according to [26, Lemma B.10], the maximum uplink achievable rate $\tilde{\mathcal{R}}_{lk}^{*}$ in (18) and optimal $\mathbf{a}_{lk}^{n*}$ in (17) can be obtained.

Corollary 1 reveals that the second-layer decoding matrix can be designed to maximize the uplink achievable rate when the first-layer decoder and data transmit power coefficients are given.

3.2 Closed-form Uplink Achievable Rate for Prior Knowledge Case

Employing MR combining as the first-layer decoder, the closed-form expression of (15) is computed for prior knowledge case as follows.

Theorem 1: *If the MMSE channel estimation and MR combining* $\boldsymbol{w}_{lk,n} = \hat{\boldsymbol{h}}_{lk,n}^{l}$ *are adopted, the uplink achievable rate of* u_{lk} *with two-layer decoding scheme can be derived in closed-form as*

$$\tilde{\mathcal{R}}_{lk}^{\mathrm{MMSE}} = (1-\frac{\tau_p}{\tau_c})\sum_{n\in\mathcal{N}}\log_2(1+\frac{\left|p_{lk}^{n}(\mathbf{a}_{lk}^{n,\mathrm{MMSE}})^{\mathrm{H}}\mathbb{E}\left\{\boldsymbol{b}_{lkk,nn}^{\mathrm{MMSE}}\right\}\right|^2}{(\mathbf{a}_{lk}^{n,\mathrm{MMSE}})^{\mathrm{H}}\left(\boldsymbol{D}_{lk}^{\mathrm{MMSE}}\right)\mathbf{a}_{lk}^{n,\mathrm{MMSE}}}), \tag{19}$$

where $\mathbb{E}\left\{\boldsymbol{b}_{lkk,nn}^{\mathrm{MMSE}}\right\} = \mathrm{diag}(\boldsymbol{Z}_{kn})$ *and*

$$\boldsymbol{D}_{lk}^{\mathrm{MMSE}} = \sum_{l''\in\mathcal{L}}\sum_{k'\in\mathcal{K}}\sum_{m\in\mathcal{N}}(p_{l''k'}^{m})^2\bar{\boldsymbol{\Gamma}}_{l''kk'}^{\mathrm{MMSE}} + \sum_{l''\in\mathcal{L}\setminus\{l\}}(p_{l''k}^{n})^2\tilde{\boldsymbol{\Gamma}}_{l''k}^{\mathrm{MMSE}} - (\boldsymbol{\Lambda}_{k,n})^2 + \boldsymbol{Z}_{kn}^{\mathrm{MMSE}}. \tag{20}$$

In (20), $\left[\boldsymbol{Z}_{kn}^{\mathrm{MMSE}}\right]_{ll}$ *is the* (l,l)th *element of* $\boldsymbol{Z}_{kn}^{\mathrm{MMSE}}$, *which can be given by* $\left[\boldsymbol{Z}_{kn}^{\mathrm{MMSE}}\right]_{ll} = \mathrm{tr}(\boldsymbol{\Omega}_{lk}^{ln} + \bar{\boldsymbol{h}}_{lk}^{ln}(\bar{\boldsymbol{h}}_{lk}^{ln})^{\mathrm{H}})$. *Moreover,* $\bar{\boldsymbol{\Gamma}}_{l''kk'}^{\mathrm{MMSE}} \in \mathbb{C}^{L\times L}$ *is a diagonal matrix with* (l,l)th *element given by*

$$\left[\bar{\boldsymbol{\Gamma}}_{l''kk'}^{\mathrm{MMSE}}\right]_{ll} = \mathrm{tr}(\lambda_{l''k'}^{lm}\boldsymbol{R}_{l''k'}^{l}\boldsymbol{\Omega}_{lk}^{ln}) + (\bar{\boldsymbol{h}}_{lk}^{ln})^{\mathrm{H}}\lambda_{l''k'}^{lm}\boldsymbol{R}_{l''k'}^{l}\bar{\boldsymbol{h}}_{lk}^{ln} + (\bar{\boldsymbol{h}}_{l''k'}^{lm})^{\mathrm{H}}\boldsymbol{\Omega}_{lk}^{ln}\bar{\boldsymbol{h}}_{l''k'}^{lm} + \left|(\bar{\boldsymbol{h}}_{lk}^{ln})^{\mathrm{H}}\bar{\boldsymbol{h}}_{l''k'}^{lm}\right|^2) \tag{21}$$

Moreover, $\boldsymbol{\Lambda}_{k,n} = \mathrm{diag}(\left|\bar{\boldsymbol{h}}_{1k}^{1n}\right|^2,...,\left|\bar{\boldsymbol{h}}_{Lk}^{Ln}\right|^2)$ *and* $\tilde{\boldsymbol{\Gamma}}_{l''k}^{\mathrm{MMSE}} = \boldsymbol{z}_{l''k}(\boldsymbol{z}_{l''k})^{\mathrm{H}}$, *where* $\boldsymbol{z}_{l''k} = \left[\mathrm{tr}(\lambda_{l''k}^{1n}\boldsymbol{R}_{l''k}^{1}(\boldsymbol{Q}_{1k}^{n})^{-1}\lambda_{1k}^{1n}\boldsymbol{R}_{1k}^{1}),...,\mathrm{tr}(\lambda_{l''k}^{Ln}\boldsymbol{R}_{l''k}^{L}(\boldsymbol{Q}_{Lk}^{n})^{-1}\lambda_{Lk}^{Ln}\boldsymbol{R}_{Lk}^{L})\right]^{\mathrm{T}}$.

Proof: Refer to Appendix A.

From Theorem 1, the following important insights into the behaviors of a multi-cell scenario with multi-antenna users over correlated Ricean fading channel is obtained.

(1) Theorem 1 is a generalized expression for analyzing the impacts of multi-antenna users, inter-cell interference, channel estimation errors and spatially correlated Ricean fading. In particular, through accordingly adjusting the parameters, this expression contains many special cases. For example, when N=1, the expression (19) denotes a uplink achievable rate expression with single-antenna users over spatially correlated Ricean fading. Moreover, if $\bar{\boldsymbol{h}}_{lk,n}^{l}$=0, then the impacts of LoS components is neglected. Under such circumstance, the expression (19) stands for an uplink achievable rate expression over spatially correlated Rayleigh fading.

(2) It is clear that the desired signal term in the numerator depends on the channel estimation accuracy and the LoS component $\bar{\boldsymbol{h}}_{lk,n}^{l}$. In fact, a larger $\bar{\boldsymbol{h}}_{lk,n}^{l}$ can significantly improve the channel estimation accuracy. Thus, a stronger LoS component makes an important contribution to enhancing the performance of system. Numerical results also validate this analysis.

(3) Moreover, Theorem 1 shows that the uplink achievable rate is seriously affected by PC term $\tilde{\boldsymbol{\Gamma}}_{l''kk'}$ in the denominator. Thus, to enhance the performance of system, the pilot decontamination schemes such as the effective power control and the optimization of second-layer decoding can be formulated by using the expression (19).

3.3 Closed-form Uplink Achievable Rate for No Prior Knowledge Case

Employing MR combining as the first-layer decoder, the closed-form expression of (15) is computed for no prior knowledge case as follows.

Theorem 2: *If the LS channel estimation and MR combining* $\boldsymbol{w}_{lk,n}=\hat{\boldsymbol{h}}_{lk,n}^{l}$ *are adopted, the uplink achievable rate of* u_{lk} *with two-layer decoding scheme is derived in closed-form as*

$$\tilde{\mathcal{R}}_{lk}^{\mathrm{LS}}=(1-\frac{\tau_p}{\tau_c})\sum_{n\in\mathcal{N}}\log_2(1+\frac{\left|p_{lk}^{n}(\mathbf{a}_{lk}^{n,\mathrm{LS}})^{\mathrm{H}}\mathbb{E}\left\{\boldsymbol{b}_{lkk,nn}^{\mathrm{LS}}\right\}\right|^2}{(\mathbf{a}_{lk}^{n,\mathrm{LS}})^{\mathrm{H}}\left(\boldsymbol{D}_{lk}^{\mathrm{LS}}\right)\mathbf{a}_{lk}^{n,\mathrm{LS}}}),\tag{22}$$

where

$$\boldsymbol{D}_{lk}^{\mathrm{LS}}=\sum_{l''\in\mathcal{L}}\sum_{k'\in\mathcal{K}}\sum_{m\in\mathcal{N}}(p_{l''k'}^{m})^2\bar{\boldsymbol{\Gamma}}_{l''kk'}^{\mathrm{LS}}-(p_{lk}^{n})^2\mathbb{E}\left\{\boldsymbol{z}_{lk}\right\}\mathbb{E}\left\{(\boldsymbol{z}_{lk})^{\mathrm{H}}\right\}+\boldsymbol{Z}_{kn}^{\mathrm{LS}}.\tag{23}$$

In (23), $\bar{\boldsymbol{\Gamma}}_{l''kk'}^{\mathrm{LS}}\in\mathbb{C}^{L\times L}$ *is a diagonal matrix with* (l,l)th *element given by*

$$\left[\bar{\boldsymbol{\Gamma}}_{l''kk'}^{\mathrm{LS}}\right]_{ll}=\mathrm{tr}(\lambda_{l''k'}^{lm}\boldsymbol{R}_{l''k'}^{lm}\boldsymbol{Q}_{lk}^{ln})+(\bar{\boldsymbol{h}}_{l''k'}^{lm})^{\mathrm{H}}\boldsymbol{Q}_{lk}^{ln}\bar{\boldsymbol{h}}_{l''k'}^{lm}+$$
$$\begin{cases}\mathrm{tr}((\lambda_{l''k}^{ln}\boldsymbol{R}_{l''k}^{ln})^2)+(\bar{\boldsymbol{y}}_{lk,n})^{\mathrm{H}}\lambda_{l''k}^{ln}\boldsymbol{R}_{l''k}^{ln}\bar{\boldsymbol{y}}_{lk,n}+\left|(\bar{\boldsymbol{c}}_{lk}^{n})^{\mathrm{H}}\bar{\boldsymbol{h}}_{l''k}^{ln}\right|^2 & \\ +\left|\mathrm{tr}(\lambda_{l''k}^{ln}\boldsymbol{R}_{l''k}^{ln})\right|^2+\left|\bar{\boldsymbol{h}}_{l''k}^{ln}\right|^4 & k'=k \text{ and } m=n \\ (\bar{\boldsymbol{y}}_{lk,n})^{\mathrm{H}}\lambda_{l''k}^{lm}\boldsymbol{R}_{l''k'}^{lm}\bar{\boldsymbol{y}}_{lk,n}+\left|(\bar{\boldsymbol{y}}_{lk,n})^{\mathrm{H}}\bar{\boldsymbol{h}}_{l''k'}^{lm}\right|^2 & \text{Otherwise.}\end{cases}\tag{24}$$

where $\bar{\boldsymbol{c}}_{lk}^{n}=\bar{\boldsymbol{y}}_{lk,n}-\bar{\boldsymbol{h}}_{l''k}^{ln}$. *In (22),* $\mathbb{E}\left\{\boldsymbol{b}_{lkk,nn}^{\mathrm{LS}}\right\}=\mathbb{E}\left\{\boldsymbol{z}_{lk}\right\}$, *where* $\boldsymbol{z}_{lk}=[\mathrm{tr}(\lambda_{lk}^{1n}\boldsymbol{R}_{lk}^{1n}+\sum_{l''\in\mathcal{L}}\bar{\boldsymbol{h}}_{l'k}^{1n}(\bar{\boldsymbol{h}}_{lk}^{1n})^{\mathrm{H}}),...,\mathrm{tr}(\lambda_{lk}^{Ln}\boldsymbol{R}_{lk}^{Ln}+\sum_{l''\in\mathcal{L}}\bar{\boldsymbol{h}}_{l'k}^{Ln}(\bar{\boldsymbol{h}}_{lk}^{Ln})^{\mathrm{H}})]^{\mathrm{H}}$. *In (23),* $\left[\boldsymbol{Z}_{kn}^{\mathrm{LS}}\right]_{ll}$ *is the* (l,l)th *element of* $\boldsymbol{Z}_{kn}$, *which can be given by* $\left[\boldsymbol{Z}_{kn}^{\mathrm{LS}}\right]_{ll}=1/\tau_p\rho_u(\mathrm{tr}(\boldsymbol{Q}_{lk}^{ln})+\left\|\bar{\boldsymbol{y}}_{lk,n}\right\|^2)$.

Proof: Refer to Appendix B.

The closed-form expression of (15) for no prior knowledge case is derived in Theorem 2, where the same insights as the observations in Theorem 1 can be easily obtained. Particularly, Theorem 2 shows that the interference terms of SINR with LS channel estimation are larger than that using MMSE channel estimation. This is because that the mean values for LS channel estimation are not used as prior information.

4. Numerical Results

In simulation, the numerical result is generated for verifying the correctness of theoretical analysis in Section 3. For a wrap-around cellular network with 4 cells, the users are uniformly and independently distributed in each cell [26]. Besides, each coherence block contains $\tau_c = 200$ samples and $\tau_p = KN$ (except Figure 7) in each cell. The LoS component from u_{lk} to the lth BS can be modeled as [27]

$$\bar{\boldsymbol{H}}_{ik}^{l} = \sqrt{\frac{\kappa_{ik}^{l}}{\kappa_{ik}^{l}+1}}\boldsymbol{\delta}_r(\theta_{ik}^{l,r})\cdot(\boldsymbol{\delta}_t(\theta_{ik}^{l,t}))^{\mathrm{T}} \tag{25}$$

where κ_{lk}^{l} =13 − 0.03d_{lk}^{l} [dB] refers to Ricean factor. d_{lk}^{l} stands for the distance between u_{lk} and the lth BS [28]. Besides, $\theta_{ik}^{l,r}$ and $\theta_{ik}^{l,t}$ denote the angle of arrival and departure. Then, $\boldsymbol{\delta}_t(\theta_{ik}^{l,t})$ and $\boldsymbol{\delta}_r(\theta_{ik}^{l,r})$ represent the transmit and receive array response vector, which can be given by [20]

$$\boldsymbol{\delta}_t(\theta_{ik}^{l,t}) = \left[1, e^{j\pi\sin(\theta_{ik}^{l,t})}, \ldots, e^{j\pi(M-1)\sin(\theta_{ik}^{l,t})}\right]^{\mathrm{T}} \tag{26}$$

$$\boldsymbol{\delta}_r(\theta_{ik}^{l,r}) = \left[1, e^{j\pi\sin(\theta_{ik}^{l,r})}, \ldots, e^{j\pi(N-1)\sin(\theta_{ik}^{l,r})}\right]^{\mathrm{T}} \tag{27}$$

Moreover, the correlation matrices $\boldsymbol{R}_{ik}^{l}$ and $\boldsymbol{U}_{ik}^{l}$ are modeled by employing the exponential correlation model from [29]. Thus, the (x,y)th and (a,b)th elements of $\boldsymbol{R}_{ik}^{l}$ and $\boldsymbol{U}_{ik}^{l}$ are given by $[\boldsymbol{R}_{ik}^{l}]_{x,y} = \rho_t e^{j(x-y)\theta_{ik}^{l,t}}$ and $[\boldsymbol{U}_{ik}^{l}]_{a,b} = \rho_r e^{j(a-b)\theta_{ik}^{l,r}}$, where ρ_t and ρ_r are correlation coefficients. In simulations, the pilot and data power is assumed to be 200mW for each user.

Fig. 2 shows the sum uplink achievable rates with the two-layer decoding when the number of BSs antennas M is increasing. The curves stand for the sum uplink achievable rate obtained by using the expressions in (19) and (22), while the "W" markers represent the sum uplink achievable rates obtained by using Monte Carlo method. It is clearly that the markers and the curves as well as simulation results are nearly overlap, which validates the correctness of our derived expressions. Particularly, spatially correlated Ricean fading channels achieve higher uplink achievable rate than the spatially correlated Rayleigh fading channels for both MMSE and LS estimation. This is because the existence of LoS component in Ricean fading channel can significantly improve achievable rate of the proposed system. Moreover, for MMSE channel estimation, the highest sum uplink achievable rates can be obtained for both the curves of analytical results and the markers. In other words, the MMSE channel estimation can achieve higher uplink achievable rate than that of LS channel estimation since the knowledge of covariance matrices is known and utilized. It can be seen from **Fig. 2**, for all cases, the sum achievable rates are steadily increasing as M grows largely.

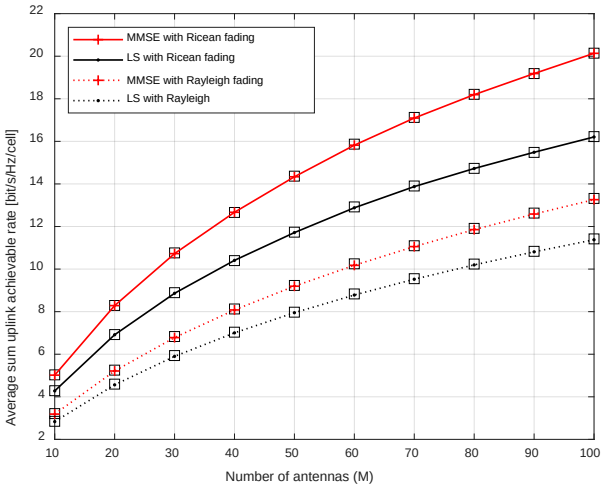

Fig. 2. Achievable rate with two-layer decoding versus the number of BS antennas ($K = 10$ and $N = 2$).

The impact of different channel estimation for uncorrelated Ricean fading is displayed in **Fig. 3**. It can be observed that the markers and the curves as well as simulation results are nearly overlap. Similar to **Fig. 2**, for the MMSE channel estimation, the highest sum uplink achievable rates can be obtained for both the curves of analytical results and the markers. This is because the mean vector of MMSE channel estimation is utilized for enhancing the accuracy of estimation. In addition, the sum achievable rate is steadily increasing for MMSE and LS channel estimators as M grows largely.

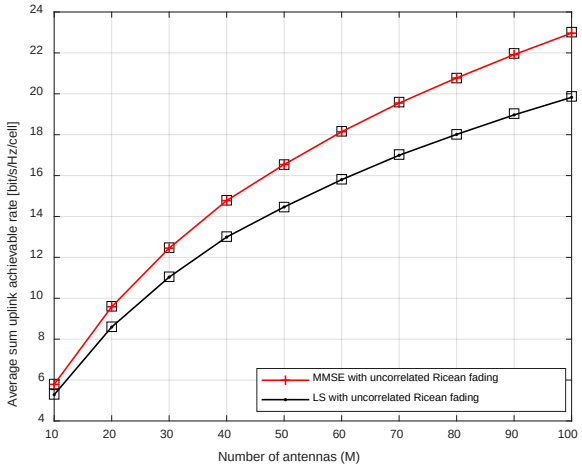

Fig. 3. Achievable rate with two-layer decoding versus the number of BS antennas for uncorrelated Ricean fading with $K = 10$ and $N = 2$.

Fig. 4 and **Fig. 5** illustrate the achievable rate comparison of the proposed two-layer precoding scheme and other precoding method for MMSE and LS channel estimation, respectively, where $K = 20$ and $N = 2$. To study the influence of two-layer decoding scheme on the uplink achievable rate, the case of approximate second-layer detector is considered, in which the second-layer detector is only computed by using the diagonal elements of the channel correlation matrices. It is clear that the two-layer decoding scheme enhance the

achievable rate with MMSE and LS channel estimation. More importantly, the LS channel estimation obtains more benefits than MMSE channel estimation does from employing the two-layer decoding scheme. This is because the two-layer decoding scheme can effectively suppress the interference caused by LS channel estimation.

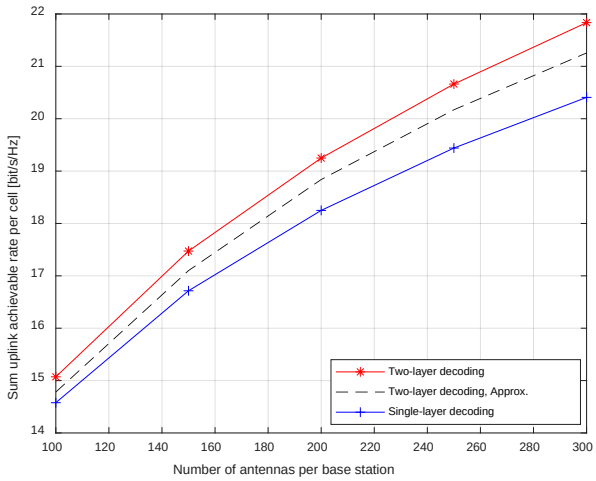

Fig. 4. Achievable rate versus M with MMSE channel estimation ($K = 20$ and $N = 2$).

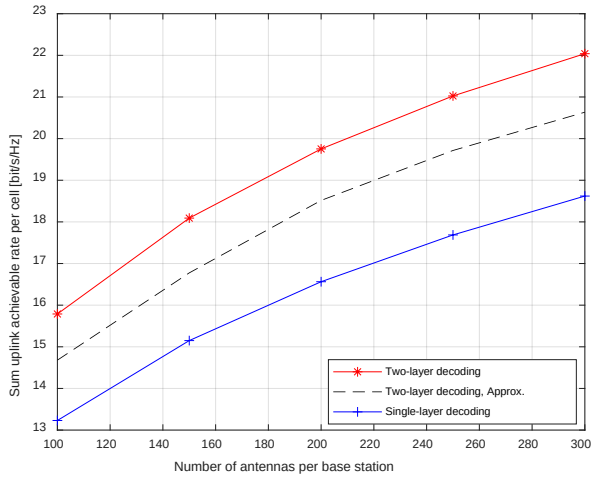

Fig. 5. Achievable rate versus M with LS channel estimation ($K = 20$ and $N = 2$).

In **Fig. 6**, the cumulative distribution function (CDF) curves for the per-user uplink achievable rate are plotted with $M = 200$, $N = 2$ and $K = 20$. It can be observed that the two-layer decoding scheme can improve the uplink achievable rate for both MMSE and LS channel estimation cases. **Fig. 6** reveals that whether the two-layer decoding scheme is adopted or not, the MMSE channel estimation can achieve higher uplink achievable rate than the LS channel estimation. In particular, LS channel estimation can achieve more benefits from two-layer decoding scheme.

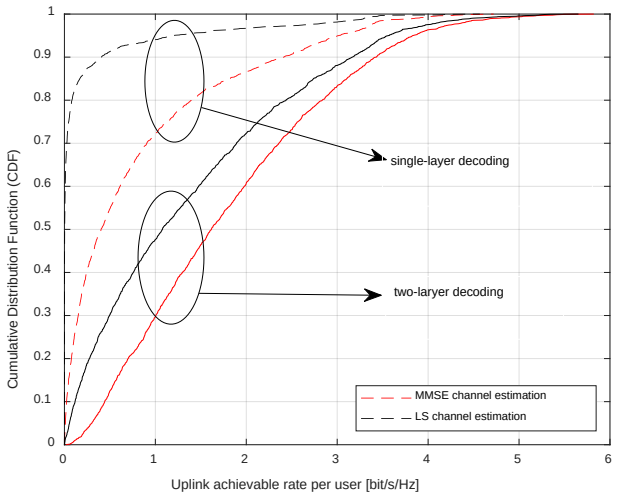

Fig. 6. CDF of per-user achievable rate for single-layer and two-layer decoding.

Fig. 7 depicts the CDF curves of per-user achievable rate for different pilot lengths, where case 1 and case 2 denote $\tau_p = 40$ and $\tau_p = 10$, respectively. For both case, the MMSE channel estimation can obtain higher uplink achievable rate than LS channel estimation. However, the CDF curve of MMSE become closer to the LS channel estimation when $\tau_p = 40$. This is because the larger pilot length can enhance the channel estimation quality, thereby mitigating the effect of PC.

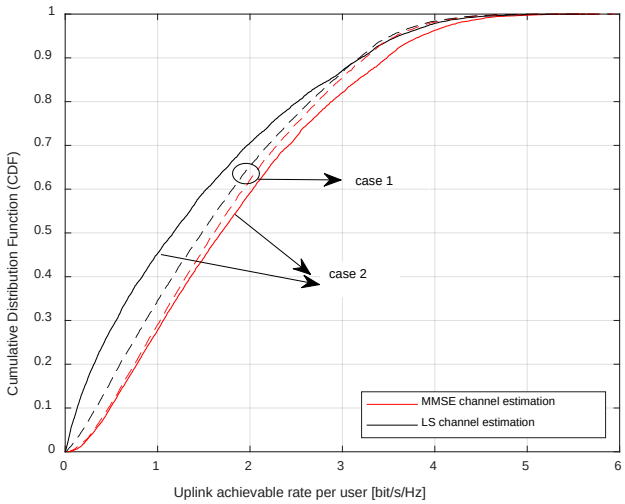

Fig. 7. CDF of per-user achievable rate with $M = 200$, $N = 2$ and $K = 20$.

In **Fig. 8**, the CDF curves of per-user achievable rate are plotted for different number of users, in which $M = 200$, $N = 2$. It reveals that the user obtains lower uplink achievable rate when the number of users increases. Moreover, as expected, the MMSE channel estimation achieves higher achievable rate than that of LS method for different number of user.

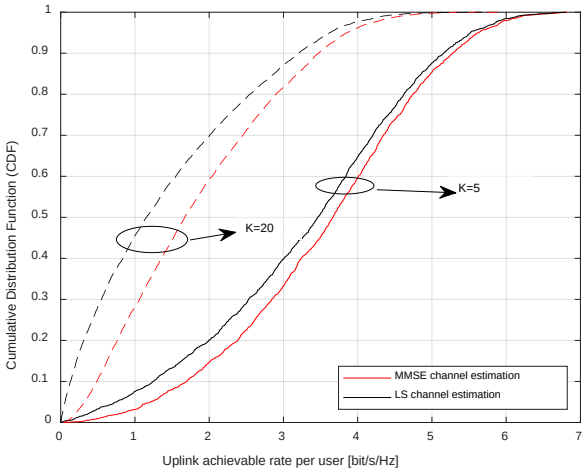

Fig. 8. CDF of the per-user achievable rate.

5. Conclusions

In this work, we investigate the uplink achievable rate of the proposed system. In such system, the channel is modeled as correlated Ricean fading. By employing two-layer decoding scheme, closed-form uplink achievable rate expressions are derived with and without prior knowledge case, respectively. These expressions can be utilized for formulating the uplink power control and other resource allocation schemes. Simulation results illustrate that the uplink achievable rate is effectively enhanced by employing two-layer decoding scheme under correlated Ricean fading channel.

Appendix A

Proof of Theorem 1

Note that $\boldsymbol{D}_{lk}$ in (16) is given by

$$\boldsymbol{D}_{lk}^{\mathrm{MMSE}} = \sum_{l''\in\mathcal{L}}\sum_{k'\in\mathcal{K}}\sum_{m\in\mathcal{N}} (p_{l''k'}^{m})^2 \bar{\boldsymbol{\Gamma}}_{l''kk'}^{\mathrm{MMSE}} + \sum_{l''=1}^{L} (p_{l''k}^{n})^2 \tilde{\boldsymbol{\Gamma}}_{l''k}^{\mathrm{MMSE}} - (p_{lk}^{n})^2 \mathbb{E}\left\{\boldsymbol{b}_{lkk,nn}^{\mathrm{MMSE}}\right\} \mathbb{E}\left\{(\boldsymbol{b}_{lkk,nn}^{\mathrm{MMSE}})^{\mathrm{H}}\right\} + \boldsymbol{Z}_{kn}^{\mathrm{MMSE}}, \quad (28)$$

where $\bar{\boldsymbol{\Gamma}}_{l''kk'}^{\mathrm{MMSE}} \in \mathbb{C}^{L\times L}$ is a diagonal matrix with (l,l)th element given by $\left[\bar{\boldsymbol{\Gamma}}_{l''kk'}^{\mathrm{MMSE}}\right]_{ll} = \mathbb{E}\left\{\left|(\boldsymbol{w}_{lk}^{n})^{\mathrm{H}} \boldsymbol{h}_{l''k'}^{lm}\right|^2\right\}$ and $\tilde{\boldsymbol{\Gamma}}_{l''k}^{\mathrm{MMSE}} = \boldsymbol{z}_{l''k}(\boldsymbol{z}_{l''k})^{\mathrm{H}}$, where $\boldsymbol{z}_{l''k} = \mathbb{E}\left[(\boldsymbol{w}_{1k}^{n})^{\mathrm{H}} \boldsymbol{h}_{l''k}^{1n}, \ldots, (\boldsymbol{w}_{Lk}^{n})^{\mathrm{H}} \boldsymbol{h}_{l''k}^{Ln}\right]^{\mathrm{T}}$.

(1) Compute $\left[\bar{\boldsymbol{\Gamma}}_{l''kk'}^{\mathrm{MMSE}}\right]_{ll} = \mathbb{E}\left\{\left|(\hat{\boldsymbol{h}}_{lk}^{ln})^{\mathrm{H}} \boldsymbol{h}_{l''k'}^{lm}\right|^2\right\}$

Case 1: $k' \neq k$ and $n \neq m$

In this case, $\hat{\boldsymbol{h}}_{lk}^{ln}$ and $\boldsymbol{h}_{l''k'}^{lm}$ are independent. Thus, $\mathbb{E}\left\{\left|(\hat{\boldsymbol{h}}_{lk}^{ln})^{\mathrm{H}} \boldsymbol{h}_{l''k'}^{lm}\right|^2\right\}$ is derived as

$$\mathbb{E}\left\{\left|(\hat{\boldsymbol{h}}_{lk}^{ln})^{\mathrm{H}} \boldsymbol{h}_{l''k'}^{lm}\right|^2\right\} = \mathrm{tr}\left(\mathbb{E}\left\{\hat{\boldsymbol{h}}_{lk}^{ln}(\hat{\boldsymbol{h}}_{lk}^{ln})^{\mathrm{H}}\right\} \mathbb{E}\left\{\boldsymbol{h}_{l''k'}^{lm}(\boldsymbol{h}_{l''k'}^{lm})^{\mathrm{H}}\right\}\right)$$

$$= \mathrm{tr}(\lambda_{l''k'}^{lm} \boldsymbol{R}_{l''k'}^{l} \boldsymbol{\Omega}_{lk}^{ln}) + (\bar{\boldsymbol{h}}_{lk}^{ln})^{\mathrm{H}} \lambda_{l''k'}^{lm} \boldsymbol{R}_{l''k'}^{l} \bar{\boldsymbol{h}}_{lk}^{ln} + (\bar{\boldsymbol{h}}_{l''k'}^{lm})^{\mathrm{H}} \boldsymbol{\Omega}_{lk}^{ln} \bar{\boldsymbol{h}}_{l''k'}^{lm} + \left|(\bar{\boldsymbol{h}}_{lk}^{ln})^{\mathrm{H}} \bar{\boldsymbol{h}}_{l''k'}^{lm}\right|^2. \quad (29)$$

Case 2: $k'=k$ and $n=m$

In this case, $\hat{\boldsymbol{h}}_{lk}^{ln}$ and $\boldsymbol{h}_{l''k}^{lm}$ are not independent. $\mathbb{E}\left\{\left|(\hat{\boldsymbol{h}}_{lk}^{ln})^{\mathrm{H}}\boldsymbol{h}_{l''k}^{lm}\right|^2\right\}$ can be derived as

$$\mathbb{E}\left\{\left|(\hat{\boldsymbol{h}}_{lk}^{ln})^{\mathrm{H}}\boldsymbol{h}_{l''k}^{ln}\right|^2\right\}=\mathbb{E}\left\{\left|(\hat{\boldsymbol{h}}_{lk}^{ln})^{\mathrm{H}}\hat{\boldsymbol{h}}_{l''k}^{ln}\right|^2\right\}+\mathbb{E}\left\{\left|(\hat{\boldsymbol{h}}_{lk}^{ln})^{\mathrm{H}}\tilde{\boldsymbol{h}}_{l''k}^{ln}\right|^2\right\}. \tag{30}$$

Using a technique proposed in [26, Lemma5], $\mathbb{E}\left\{\left|(\hat{\boldsymbol{h}}_{lk}^{ln})^{\mathrm{H}}\hat{\boldsymbol{h}}_{l''k}^{ln}\right|^2\right\}$ can be derived as

$$\begin{aligned}\mathbb{E}\left\{\left|(\hat{\boldsymbol{h}}_{lk}^{ln})^{\mathrm{H}}\hat{\boldsymbol{h}}_{l''k}^{ln}\right|^2\right\}&=\mathrm{tr}((\lambda_{l''k}^{ln}\boldsymbol{R}_{l''k}^{l}-\boldsymbol{C}_{l''k}^{ln})\boldsymbol{\Omega}_{lk}^{ln})+\left|\mathrm{tr}(\lambda_{l''k}^{ln}\boldsymbol{R}_{l''k}^{l}(\boldsymbol{Q}_{lk}^{n})^{-1}\lambda_{lk}^{ln}\boldsymbol{R}_{lk}^{l})\right|^2+\left|(\bar{\boldsymbol{h}}_{lk}^{ln})^{\mathrm{H}}\bar{\boldsymbol{h}}_{l''k}^{ln}\right|^2\\&\quad+(\bar{\boldsymbol{h}}_{lk}^{ln})^{\mathrm{H}}(\lambda_{l''k,n}^{l}\boldsymbol{R}_{l''k}^{l}-\boldsymbol{C}_{l''k}^{ln})\bar{\boldsymbol{h}}_{lk}^{ln}+(\bar{\boldsymbol{h}}_{l''k}^{ln})^{\mathrm{H}}\boldsymbol{\Omega}_{lk}^{ln}\bar{\boldsymbol{h}}_{l''k}^{ln}.\end{aligned} \tag{31}$$

Note that $\tilde{\boldsymbol{h}}_{l''k}^{ln}$ and $\hat{\boldsymbol{h}}_{lk}^{ln}$ in (30) are independent, $\mathbb{E}\left\{\left|(\hat{\boldsymbol{h}}_{lk}^{ln})^{\mathrm{H}}\tilde{\boldsymbol{h}}_{l''k}^{ln}\right|^2\right\}$ can be computed as

$$\begin{aligned}\mathbb{E}\left\{\left|(\hat{\boldsymbol{h}}_{lk}^{ln})^{\mathrm{H}}\tilde{\boldsymbol{h}}_{l''k}^{ln}\right|^2\right\}&=\mathbb{E}\left\{(\hat{\boldsymbol{h}}_{lk}^{ln})^{\mathrm{H}}\tilde{\boldsymbol{h}}_{l''k}^{ln}(\tilde{\boldsymbol{h}}_{l''k}^{ln})^{\mathrm{H}}\hat{\boldsymbol{h}}_{lk}^{ln}\right\}\\&=\mathrm{tr}(\boldsymbol{C}_{l''k}^{ln}\boldsymbol{\Omega}_{lk}^{ln})+(\bar{\boldsymbol{h}}_{lk}^{ln})^{\mathrm{H}}(\boldsymbol{C}_{l''k}^{ln})\bar{\boldsymbol{h}}_{lk}^{ln}.\end{aligned} \tag{32}$$

Note that $\hat{\boldsymbol{h}}_{lk}^{ln}$ and $\boldsymbol{h}_{l'k'}^{lm}$ are independent for other cases. Thereby, $\mathbb{E}\left\{\left|(\hat{\boldsymbol{h}}_{lk}^{ln})^{\mathrm{H}}\boldsymbol{h}_{l'k'}^{lm}\right|^2\right\}$ can be easily obtained for other cases by employing the similar approach in (29).

Then, combining all case, $\left[\bar{\boldsymbol{\Gamma}}_{l''kk'}^{\mathrm{MMSE}}\right]_{ll}$ can be written as

$$\begin{aligned}\left[\bar{\boldsymbol{\Gamma}}_{l''kk'}^{\mathrm{MMSE}}\right]_{ll}&=\mathbb{E}\left\{\left|(\hat{\boldsymbol{h}}_{lk}^{ln})^{\mathrm{H}}\boldsymbol{h}_{l''k'}^{lm}\right|^2\right\}\\&=\mathrm{tr}(\lambda_{l''k'}^{lm}\boldsymbol{R}_{l''k'}^{l}\boldsymbol{\Omega}_{lk}^{ln})+(\bar{\boldsymbol{h}}_{lk}^{ln})^{\mathrm{H}}\lambda_{l''k'}^{lm}\boldsymbol{R}_{l''k'}^{l}\bar{\boldsymbol{h}}_{lk}^{ln}+(\bar{\boldsymbol{h}}_{l''k'}^{lm})^{\mathrm{H}}\boldsymbol{\Omega}_{lk}^{ln}\bar{\boldsymbol{h}}_{l''k'}^{lm}+\left|(\bar{\boldsymbol{h}}_{lk}^{ln})^{\mathrm{H}}\bar{\boldsymbol{h}}_{l''k'}^{lm}\right|^2+\\&\quad\begin{cases}\left|\mathrm{tr}(\lambda_{l''kn}^{ln}\boldsymbol{R}_{l''k}^{l}(\boldsymbol{Q}_{lk}^{n})^{-1}\lambda_{lk}^{ln}\boldsymbol{R}_{lk}^{l})\right|^2 & k'=k,m=n\\0 & \text{Otherwise.}\end{cases}\end{aligned} \tag{33}$$

(2) Compute $\tilde{\boldsymbol{\Gamma}}_{l''k}^{\mathrm{MMSE}}$

$$\tilde{\boldsymbol{\Gamma}}_{l''k}^{\mathrm{MMSE}}=\begin{bmatrix}\Sigma_{l''k}^{11n} & \cdots & \Sigma_{l''k}^{1Ln}\\ \vdots & \ddots & \vdots\\ \Sigma_{l''k}^{L1n} & \cdots & \Sigma_{l''k}^{LLn}\end{bmatrix} \tag{34}$$

where $\Sigma_{l''k}^{ll'n}=\mathbb{E}\left\{(\boldsymbol{w}_{lk}^{n})^{\mathrm{H}}\boldsymbol{h}_{l''k'}^{lm}\right\}\mathbb{E}\left\{(\boldsymbol{w}_{l'k}^{n})^{\mathrm{H}}\boldsymbol{h}_{l''k}^{l'n}\right\}$

Case 1: $l\neq l'$

$$\mathbb{E}\left\{(\hat{\boldsymbol{h}}_{lk}^{ln})^{\mathrm{H}}\boldsymbol{h}_{l''k}^{ln}\right\}\mathbb{E}\left\{(\hat{\boldsymbol{h}}_{l'k}^{l'n})^{\mathrm{H}}\boldsymbol{h}_{l''k}^{l'n}\right\}=\boldsymbol{z}_{l''k}(\boldsymbol{z}_{l''k})^{\mathrm{H}}, \tag{35}$$

where $\boldsymbol{z}_{l''k}=\left[\mathrm{tr}(\lambda_{l''k}^{1n}\boldsymbol{R}_{l''k}^{1}(\boldsymbol{Q}_{1k}^{n})^{-1}\lambda_{1k}^{1n}\boldsymbol{R}_{1k}^{1}),\ldots,\mathrm{tr}(\lambda_{l''k}^{Ln}\boldsymbol{R}_{l''k}^{L}(\boldsymbol{Q}_{Lk}^{n})^{-1}\lambda_{Lk}^{Ln}\boldsymbol{R}_{Lk}^{L})\right]^{\mathrm{T}}$

Case 2: $l=l'$

$$\mathbb{E}\left\{(\hat{\boldsymbol{h}}_{lk}^{ln})^{\mathrm{H}}\boldsymbol{h}_{l''k}^{ln}(\hat{\boldsymbol{h}}_{lk}^{ln})^{\mathrm{H}}\boldsymbol{h}_{l''k}^{ln}\right\}=\mathbb{E}\left\{\boldsymbol{b}_{l''kk,nn}\right\}\mathbb{E}\left\{(\boldsymbol{b}_{l''kk,nn})^{\mathrm{H}}\right\}-(\boldsymbol{\Lambda}_{k,n})^2, \tag{36}$$

where $\boldsymbol{\Lambda}_{k,n}=\mathrm{diag}(\left|\bar{\boldsymbol{h}}_{1k}^{1n}\right|^2,\ldots,\left|\bar{\boldsymbol{h}}_{Lk}^{Ln}\right|^2)$.

Then, combining (35) and (36), $\tilde{\boldsymbol{\Gamma}}_{l''k}^{\mathrm{MMSE}}$ can be written as

$$\tilde{\boldsymbol{\Gamma}}_{l''kk'}=\begin{cases}\boldsymbol{z}_{l''k}(\boldsymbol{z}_{l''k})^{\mathrm{H}}, & \text{case 1,}\\ \mathbb{E}\left\{\boldsymbol{b}_{l''kk,nn}\right\}\mathbb{E}\left\{(\boldsymbol{b}_{l''kk,nn})^{\mathrm{H}}\right\}-(\boldsymbol{\Lambda}_{k,n})^{2}, & \text{case 2.}\end{cases} \tag{37}$$

(3) Compute $\boldsymbol{Z}_{kn}^{\mathrm{MMSE}}$

$$\begin{aligned}\left[\boldsymbol{Z}_{kn}^{\mathrm{MMSE}}\right]_{ll}&=\mathbb{E}\left\{\left\|\boldsymbol{w}_{lk}^{n}\right\|^{2}\right\}\\&=\mathrm{tr}(\boldsymbol{\Omega}_{lk}^{ln}+\bar{\boldsymbol{h}}_{lk}^{ln}(\bar{\boldsymbol{h}}_{lk}^{ln})^{\mathrm{H}}).\end{aligned} \tag{38}$$

(4) Compute $\mathbb{E}\left\{\boldsymbol{b}_{lkk,nn}^{\mathrm{MMSE}}\right\}$

$$\begin{aligned}\mathbb{E}\left\{\boldsymbol{b}_{lkk,nn}^{\mathrm{MMSE}}\right\}&=\mathbb{E}\left\{\left[(\boldsymbol{w}_{1k}^{n})^{\mathrm{H}}\boldsymbol{h}_{lk}^{1n},\ldots,(\boldsymbol{w}_{Lk}^{n})^{\mathrm{H}}\boldsymbol{h}_{lk}^{Ln}\right]^{\mathrm{T}}\right\}\\&=\mathrm{diag}(\boldsymbol{Z}_{kn}^{\mathrm{MMSE}})\end{aligned} \tag{39}$$

Finally, substituting (33), (37) and (39) into (16), the desired uplink achievable rate can be obtained in (19).

Appendix B

Proof of Theorem 2

Similar to Theorem 1, $\bar{\boldsymbol{\Gamma}}_{l''kk'}^{\mathrm{LS}}$, $\tilde{\boldsymbol{\Gamma}}_{l''k}^{\mathrm{LS}}$, $\boldsymbol{Z}_{kn}^{\mathrm{LS}}$, and $\mathbb{E}\left\{\boldsymbol{b}_{lkk,nn}^{\mathrm{LS}}\right\}$ are needed to be computed as follows.

(1) Compute $\left[\bar{\boldsymbol{\Gamma}}_{l''kk'}^{\mathrm{LS}}\right]_{ll}=\mathbb{E}\left\{\left|(\hat{\boldsymbol{h}}_{lk}^{ln})^{\mathrm{H}}\boldsymbol{h}_{l''k'}^{lm}\right|^{2}\right\}$

Note that $\hat{\boldsymbol{h}}_{lk}^{ln,\mathrm{LS}}=(1/\tau_p\sqrt{\rho_u})\,\hat{\boldsymbol{y}}_{lk,n}$, $\hat{\boldsymbol{y}}_{lk,n}=\sum_{l'\in\mathcal{L}}\boldsymbol{h}_{l'k}^{ln}+\boldsymbol{n}_{l'k}$, and $\hat{\boldsymbol{y}}_{lk,n}\sim\mathcal{CN}\left(\bar{\boldsymbol{y}}_{lk,n},\tau_p\boldsymbol{Q}_{lk}^{ln}\right)$. For case 1 ($m\neq n$ and $k'=k$), case 2 ($k'\neq k$ and $m=n$), and case 3($k'\neq k$ and $m\neq n$), $\boldsymbol{h}_{l''k'}^{lm}$ and $\hat{\boldsymbol{y}}_{lk,n}$ are independent. Thus,

$$\begin{aligned}\mathbb{E}\left\{\left|(\hat{\boldsymbol{y}}_{lk,n})^{\mathrm{H}}\boldsymbol{h}_{l''k'}^{lm}\right|^{2}\right\}&=\mathbb{E}\left\{(\hat{\boldsymbol{y}}_{lk,n})^{\mathrm{H}}\boldsymbol{h}_{l''k'}^{lm}(\boldsymbol{h}_{l''k'}^{lm})^{\mathrm{H}}\hat{\boldsymbol{y}}_{lk,n}\right\}\\&=\mathrm{tr}(\lambda_{l''k}^{lm}\boldsymbol{R}_{l''k'}^{l}\boldsymbol{Q}_{lk}^{ln})+(\bar{\boldsymbol{y}}_{lk,n})^{\mathrm{H}}\lambda_{l''k}^{lm}\boldsymbol{R}_{l''k'}^{l}\bar{\boldsymbol{y}}_{lk,n}+(\bar{\boldsymbol{h}}_{l''k'}^{lm})^{\mathrm{H}}\boldsymbol{Q}_{lk}^{ln}\bar{\boldsymbol{h}}_{l''k'}^{lm}+\left|(\bar{\boldsymbol{y}}_{lk,n})^{\mathrm{H}}\bar{\boldsymbol{h}}_{l''k'}^{lm}\right|^{2}.\end{aligned} \tag{40}$$

Case 4: $k'=k$ and $m=n$.

In this case, $\hat{\boldsymbol{h}}_{lk}^{ln}$ and $\boldsymbol{h}_{l''k'}^{lm}$ are not independent. Define that $\boldsymbol{c}_{lk}^{n}=\hat{\boldsymbol{y}}_{lk,n}-\boldsymbol{h}_{l''k}^{ln}$, then $\boldsymbol{c}_{lk}^{n}\sim\mathcal{CN}\left(\bar{\boldsymbol{c}}_{lk}^{n},\boldsymbol{\Xi}_{lk}^{ln}\right)$, where $\bar{\boldsymbol{c}}_{lk}^{n}=\bar{\boldsymbol{y}}_{lk,n}-\bar{\boldsymbol{h}}_{l''k}^{ln}$ and $\boldsymbol{\Xi}_{lk}^{ln}=\dfrac{1}{\tau_p\rho_u}\boldsymbol{Q}_{lk}^{ln}-\boldsymbol{R}_{l''k}^{l}\lambda_{l''k}^{ln}$. Then $\mathbb{E}\left\{\left|(\hat{\boldsymbol{y}}_{lk,n})^{\mathrm{H}}\boldsymbol{h}_{l''k'}^{lm}\right|^{2}\right\}$ can be approximated as

$$\mathbb{E}\left\{\left|(\hat{\boldsymbol{y}}_{lk,n})^{\mathrm{H}}\boldsymbol{h}_{l''k'}^{lm}\right|^{2}\right\}=\mathbb{E}\left\{\left|(\boldsymbol{c}_{lk}^{n})^{\mathrm{H}}\boldsymbol{h}_{l''k}^{ln})\right|^{2}\right\}+\mathbb{E}\left\{\left|(\boldsymbol{h}_{l''k}^{ln})^{\mathrm{H}}\boldsymbol{h}_{l''k}^{ln}\right|^{2}\right\}. \tag{41}$$

Note that $\boldsymbol{c}_{lk}^{n}$ is independent of $\boldsymbol{h}_{l''k}^{ln}$, thus

$$\mathbb{E}\left\{\left|(\boldsymbol{c}_{lk}^{n})^{\mathrm{H}}\boldsymbol{h}_{l''k}^{ln})\right|^{2}\right\}=\mathrm{tr}(\lambda_{l''k}^{ln}\boldsymbol{R}_{l''k}^{l}\boldsymbol{\Xi}_{lk}^{ln})+(\bar{\boldsymbol{c}}_{lk}^{n})^{\mathrm{H}}\lambda_{l''k}^{ln}\boldsymbol{R}_{l''k}^{l}\bar{\boldsymbol{c}}_{lk}^{n}+(\bar{\boldsymbol{h}}_{l''k}^{ln})^{H}\boldsymbol{\Xi}_{lk}^{ln}\bar{\boldsymbol{h}}_{l''k}^{ln}+\left|(\bar{\boldsymbol{c}}_{lk}^{n})^{\mathrm{H}}\bar{\boldsymbol{h}}_{l''k}^{ln}\right|^{2}. \tag{42}$$

Using the proposed technology in [26, Lemma4], $\mathbb{E}\left\{\left|(\boldsymbol{h}_{l''k}^{ln})^{\mathrm{H}}\boldsymbol{h}_{l''k}^{ln}\right|^{2}\right\}$ is computed as

$$\begin{aligned}\mathbb{E}\left\{\left|(\boldsymbol{h}_{lk}^{ln})^{\mathrm{H}}\boldsymbol{h}_{lk}^{ln}\right|^{2}\right\}&=\left|\mathrm{tr}(\lambda_{l''k}^{ln}\boldsymbol{R}_{l''k}^{l})\right|^{2}+\mathrm{tr}((\lambda_{l''k}^{ln}\boldsymbol{R}_{l''k}^{l})^{2})+\\&\quad 2\left|\bar{\boldsymbol{h}}_{l''k}^{ln}\right|^{2}\mathrm{tr}(\lambda_{l''k}^{ln}\boldsymbol{R}_{l''k}^{l})+2(\bar{\boldsymbol{h}}_{l''k}^{ln})^{\mathrm{H}}\lambda_{l''k}^{ln}\boldsymbol{R}_{l''k}^{l}\bar{\boldsymbol{h}}_{l''k}^{ln}+\left|\bar{\boldsymbol{h}}_{l''k}^{ln}\right|^{4}).\end{aligned} \tag{43}$$

Then, combining all case, $\left[\overline{\boldsymbol{\Gamma}}_{l''kk'}^{\mathrm{LS}}\right]_{ll}$ can be written as

$$\begin{aligned}\left[\overline{\boldsymbol{\Gamma}}_{l''kk'}^{\mathrm{LS}}\right]_{ll} &= \mathbb{E}\left\{\left|(\hat{\boldsymbol{h}}_{lk}^{ln})^{\mathrm{H}}\boldsymbol{h}_{l''k'}^{lm}\right|^2\right\} \\ &= \mathrm{tr}(\lambda_{l''k}^{lm}\boldsymbol{R}_{l''k'}^{l}\boldsymbol{Q}_{lk}^{ln}) + (\overline{\boldsymbol{h}}_{l''k'}^{lm})^{\mathrm{H}}\boldsymbol{Q}_{lk}^{ln}\overline{\boldsymbol{h}}_{l''k'}^{lm} \\ &\quad \begin{cases} +\mathrm{tr}((\lambda_{l''k}^{ln}\boldsymbol{R}_{l''k}^{l})^2) + (\overline{\boldsymbol{y}}_{lk,n})^{\mathrm{H}}\lambda_{l''k}^{ln}\boldsymbol{R}_{l''k}^{l}\overline{\boldsymbol{y}}_{lk,n} + \left|(\overline{\boldsymbol{c}}_{lk}^{n})^{\mathrm{H}}\overline{\boldsymbol{h}}_{l''k}^{ln}\right|^2 \\ +\left|\mathrm{tr}(\lambda_{l''k}^{ln}\boldsymbol{R}_{l''k}^{l})\right|^2 + \left|\overline{\boldsymbol{h}}_{l''k}^{ln}\right|^4 \qquad \text{case 4} \\ +(\overline{\boldsymbol{y}}_{lk,n})^{\mathrm{H}}\lambda_{l''k}^{ln}\boldsymbol{R}_{l''k'}^{l}\overline{\boldsymbol{y}}_{lk,n} + \left|(\overline{\boldsymbol{y}}_{lk,n})^{\mathrm{H}}\overline{\boldsymbol{h}}_{l''k'}^{lm}\right|^2 \quad \text{Otherwise.} \end{cases} \end{aligned} \tag{44}$$

(2) Compute $\tilde{\boldsymbol{\Gamma}}_{l''k}^{\mathrm{LS}}$

1) If $l \neq l'$,

$$\begin{aligned}\mathbb{E}\left\{(\hat{\boldsymbol{h}}_{lk}^{ln})^{\mathrm{H}}\boldsymbol{h}_{l''k}^{ln}(\hat{\boldsymbol{h}}_{l'k}^{l'n})^{\mathrm{H}}\boldsymbol{h}_{l''k}^{l'n}\right\} &= \mathrm{tr}(\lambda_{l''k}^{ln}\boldsymbol{R}_{l''k}^{l} + \sum_{l'\in\mathcal{L}}\overline{\boldsymbol{h}}_{l''k}^{ln}(\overline{\boldsymbol{h}}_{l''k}^{ln})^{\mathrm{H}})\mathrm{tr}(\lambda_{l''k}^{l'n}\boldsymbol{R}_{l''k}^{l'} + \sum_{l'''\in\mathcal{L}}\overline{\boldsymbol{h}}_{l'''k}^{l'n}(\overline{\boldsymbol{h}}_{l'''k}^{l'n})^{\mathrm{H}}) \\ &= \boldsymbol{z}_{l''k}(\boldsymbol{z}_{l''k})^{\mathrm{H}}, \end{aligned} \tag{45}$$

where $\boldsymbol{z}_{l''k} = \left[\mathrm{tr}(\lambda_{l''k}^{1n}\boldsymbol{R}_{l''k}^{1} + \sum_{l'\in\mathcal{L}}\overline{\boldsymbol{h}}_{l''k}^{1n}(\overline{\boldsymbol{h}}_{l''k}^{1n})^{\mathrm{H}}),\ldots,\mathrm{tr}(\lambda_{l''k}^{Ln}\boldsymbol{R}_{l''k}^{L} + \sum_{l'\in\mathcal{L}}\overline{\boldsymbol{h}}_{l''k}^{Ln}(\overline{\boldsymbol{h}}_{l''k}^{Ln})^{\mathrm{H}})\right]^{\mathrm{T}}$.

2) If $l = l'$, similar to (36),

$$\mathbb{E}\left\{(\hat{\boldsymbol{h}}_{lk}^{ln})^{\mathrm{H}}\boldsymbol{h}_{l''k}^{ln}(\hat{\boldsymbol{h}}_{lk}^{ln})^{\mathrm{H}}\boldsymbol{h}_{l''k}^{ln}\right\} = \mathbb{E}\left\{\boldsymbol{b}_{l''kk,nn}^{\mathrm{LS}}\right\}\mathbb{E}\left\{(\boldsymbol{b}_{l''kk,nn}^{\mathrm{LS}})^{\mathrm{H}}\right\} - (\boldsymbol{\Lambda}_{k,n})^2, \tag{46}$$

(3) Compute $\boldsymbol{Z}_{kn}^{\mathrm{LS}}$

$$\begin{aligned}\left[\boldsymbol{Z}_{kn}^{\mathrm{LS}}\right]_{ll} &= \mathbb{E}\left\{\left\|\boldsymbol{w}_{lk}^{n}\right\|^2\right\} \\ &= \frac{1}{\tau_p\rho_u}(\mathrm{tr}(\boldsymbol{Q}_{lk}^{ln}) + \left\|\overline{\boldsymbol{y}}_{lk,n}\right\|^2). \end{aligned} \tag{47}$$

(4) Compute $\mathbb{E}\left\{\boldsymbol{b}_{lkk,nn}^{\mathrm{LS}}\right\}$

$$\begin{aligned}\mathbb{E}\left\{\boldsymbol{b}_{lkk,nn}^{\mathrm{LS}}\right\} &= \mathbb{E}\left\{\left[(\boldsymbol{w}_{1k}^{n})^{\mathrm{H}}\boldsymbol{h}_{lk}^{1n},\ldots,(\boldsymbol{w}_{Lk}^{n})^{\mathrm{H}}\boldsymbol{h}_{lk}^{Ln}\right]^{\mathrm{T}}\right\} \\ &= \mathbb{E}\left[\mathrm{tr}(\lambda_{lk}^{1n}\boldsymbol{R}_{lk}^{1} + \sum_{l'\in\mathcal{L}}\overline{\boldsymbol{h}}_{l'k}^{1n}(\overline{\boldsymbol{h}}_{lk}^{1n})^{\mathrm{H}}),\ldots,\ \mathrm{tr}(\lambda_{lk}^{Ln}\boldsymbol{R}_{lk}^{L} + \sum_{l'\in\mathcal{L}}\overline{\boldsymbol{h}}_{l'k}^{Ln}(\overline{\boldsymbol{h}}_{lk}^{Ln})^{\mathrm{H}})\right]^{\mathrm{T}} \\ &= \mathbb{E}\left\{\boldsymbol{z}_{lk}\right\} \end{aligned} \tag{48}$$

Finally, substituting (44), (47) and (48) into (16), the desired uplink achievable rate can be obtained in (22).

References

[1] J. Zhang, E. Björnson, M. Matthaiou, D. W. K. Ng, H. Yang, and D. J. Love, "Prospective multiple antenna technologies for beyond 5G," *IEEE Journal on Selected Areas in Communications*, vol. 38, no. 8, pp. 1637–1660, Aug. 2020. Article (CrossRef Link)

[2] K. Xu, Z. X. Shen, Y. R. Wang, and X. C. Xia, "Hybrid time-switching and power splitting SWIPT for full-duplex massive MIMO systems: a beam-domain approach," *IEEE Transactions on Vehicular Technology*, vol. 67, no. 8, pp. 7257-7274, Aug. 2018. Article (CrossRef Link)

[3] Z. X. Shen, K. Xu, X. C. Xia, and W. Xie, "Spatial sparsity based secure transmission strategy for massive MIMO systems against simultaneous jamming and eavesdropping," *IEEE Transactions on Information Forensics and Security*, vol. 15, pp. 3760-3774, Jun. 2020. Article (CrossRef Link)

[4] K. Xu, Z. X. Shen, Y. R. Wang, and X. C. Xia, "Location-aided mMIMO channel tracking and hybrid beamforming for high-speed railway communications: an angle-domain approach," *IEEE Systems Journal*, vol. 14, no. 1, pp. 93-104, Mar. 2020. Article (CrossRef Link)
[5] Z. Bao, Y. Lin, S. Zhang, Z. Li, and S. Mao, "Threat of Adversarial Attacks on DL-Based IoT Device Identification," *IEEE Internet of Things Journal*, vol. 9, no. 11, pp. 9012-9024, Jun. 2022. Article (CrossRef Link)
[6] Y. Tu, Y. Lin, and H. Zha, "Large-scale real-world radio signal recognition with deep learning," *Chinese Journal of Aeronautics*, vol. 35, no. 9, pp. 35-48, Sep. 2022. Article (CrossRef Link)
[7] T. C. Mai, H. Quoc Ngo, and T. Q. Duong, "Cell-free massive MIMO systems with multi-antenna users," in *Proc. of IEEE Global Conference on Signal and Information Processing (GlobalSIP)*, pp. 828–832, 2018. Article (CrossRef Link)
[8] Z. Wang, J. Zhang, B. Ai, C. Yuen, and M. Debbah, "Uplink performance of cell-free massive MIMO with multi-antenna users over jointly-correlated Rayleigh fading channels," *IEEE Transactions on Wireless Communications*, vol. 21, no. 9, pp. 7391-7406, Sep.2022. Article (CrossRef Link)
[9] X. Li, J. Zhang, Z. Wang, B. Ai, and D. W. K. Ng, "Cell-free massive MIMO with multi-antenna users over weichselberger Rician channels," *IEEE Transactions on Vehicular Technology*, vol. 71, no. 11, pp. 12368-12373, Nov. 2022. Article (CrossRef Link)
[10] T. C. Mai, H. Q. Ngo, and T. Q. Duong, "Downlink spectral efficiency of cell-free massive MIMO systems with multi-antenna users," *IEEE Transactions on Communications*, vol. 68, no. 8, pp. 4803-4815, Aug. 2020. Article (CrossRef Link)
[11] X. Li, E. Björnson, S. Zhou, and J. Wang, "Massive MIMO with multiantenna users: when are additional user antennas beneficial?," in *Proc. of 23rd International Conference on Telecommunications (ICT)*, pp. 1–6, 2016. Article (CrossRef Link)
[12] X. Wu and D. Liu, "Novel insight into multi-user channels with multi-antenna users," *IEEE Communications Letters*, vol. 21, no. 9, pp. 1961-1964, Sept. 2017. Article (CrossRef Link)
[13] F. Rezaei and A. Tadaion, "Multi-layer beamforming in uplink/downlink massive MIMO systems with multi-antenna users," *Signal Process.*, vol. 164, pp. 58–66, Nov. 2019. Article (CrossRef Link)
[14] J. A. Sutton, H. Q. Ngo, and M. Matthaiou, "Performance of a novel maximum-ratio precoder in massive MIMO with multiple-antenna users," in *Proc. of IEEE 30th Annual International Symposium on Personal, Indoor and Mobile Radio Communications (PIMRC)*, pp. 1–6, 2019. Article (CrossRef Link)
[15] J. A. C. Sutton, H. Q. Ngo, and M. Matthaiou, "Hardening the channels by precoder design in massive MIMO with multiple-antenna users," *IEEE Transactions on Vehicular Technology*, vol. 70, no. 5, pp. 4541-4556, May 2021. Article (CrossRef Link)
[16] M. Maleki, K. Mohamed-Pour, and M. Soltanalian, "Large-system mutual information analysis of receive spatial modulation in correlated multi-cell massive MIMO networks," *IEEE Transactions on Communications*, vol. 67, no. 9, pp. 6071-6084, Sept. 2019. Article (CrossRef Link)
[17] H. Mohammadghasemi, M. F. Sabahi, and A. R. Forouzan, "Pilot-decontamination in massive MIMO systems using interference alignment," *IEEE Communications Letters*, vol. 24, no. 3, pp. 672-675, Mar. 2020. Article (CrossRef Link)
[18] L. He, J. T. Wang, J. Song, and L. Hanzo, "On the multi-user multi-Cell Massive Spatial Modulation Uplink: How Many Antennas for Each User?," *IEEE Transactions on Wireless Communications*, vol. 16, no. 3, pp. 1437−1451, Mar. 2017. Article (CrossRef Link)
[19] Z. Wang, J. Zhang, E. Björnson, and B. Ai, "Uplink performance of cell-free massive MIMO over spatially correlated Rician fading channels," *IEEE Communications Letters*, vol. 25, no. 4, pp. 1348-1352, April 2021. Article (CrossRef Link)
[20] K. Dovelos, M. Matthaiou, H. Q. Ngo, and B. Bellalta, "Massive MIMO with multi-antenna users under jointly correlated Ricean fading," in *Proc. of 2020 IEEE International Conference on Communications (ICC)*, pp. 1–6, 2020. Article (CrossRef Link)

[21] T. V. Chien, C. Mollén, and E. Björnson, "Large-scale-fading decoding in cellular massive MIMO systems with spatially correlated channels," *IEEE Transactions on Communications*, vol. 67, no. 4, pp. 2746 - 2762, Apr. 2019. Article (CrossRef Link)

[22] A. Adhikary, A. Ashikhmin, and T. L. Marzetta, "Uplink interference reduction in large-scale antenna systems," *IEEE Transactions on Communications*, vol. 65, no. 5, pp. 2194-2206, May 2017. Article(CrossRef Link)

[23] D. Kudathanthirige and G. Amarasuriya, "Distributed massive MIMO downlink," in *Proc. of 2019 IEEE International Conference on Communications (ICC)*, pp. 1-7, 2019. Article (CrossRef Link)

[24] S. M. Kay, *Fundamentals of statistical signal processing: estimation theory*, Upper Saddle River, 1993. Article (CrossRef Link)

[25] Ö. Özdogan, E. Björnson, and E. G. Larsson, "Massive MIMO with spatially correlated Rician fading channels," *IEEE Transactions on Communications*, vol. 67, no. 5, pp. 3234-3250, May 2019. Article (CrossRef Link)

[26] E. Björnson, J. Hoydis, and L. Sanguinetti, "Massive MIMO Networks: Spectral, Energy, and Hardware Efficiency," *Found. Trends Signal Process.*, vol. 11, no. 3-4, pp. 154-655, Nov. 2017. Article (CrossRef Link)

[27] A. G. Burr, "Capacity bounds and estimates for the finite scatterers MIMO wireless channel," *IEEE Journal on Selected Areas in Communications*, vol. 21, no. 5, pp. 812-818, Jun. 2003. Article (CrossRef Link)

[28] Technical Specification Group Radio Access Network; Spatial Channel Model for Multiple Input Multiple Output (MIMO) Simulations, document 3GPP TR 25.996 V14.0.0, 3rd Generation Partnership Project, Mar. 2017.

[29] S. L. Loyka, "Channel capacity of MIMO architecture using the exponential correlation matrix," *IEEE Communications Letters*, vol. 5, no. 9, pp. 369-371, Sept. 2001. Article (CrossRef Link)

Yixin Xu was born in Hebei, china, in 1981. He received the M.S. degree from Yanshan University, Qinhuangdao, china, in 2011. He is currently pursuing the Ph.D. degree in signal and information processing with Northeastern University. His research interest includes signal processing for communications and Massive MIMO.

Fulai Liu was born in Hebei, China, in 1975. He received the M.S. degree and the Ph.D. degree from Northeastern University, Shenyang, China, in 2002 and 2005, respectively. Since 2010, he is a professor at Northeastern University, Qinhuangdao, China. His research interests include array signal processing and its applications, cognitive radio, etc.

Zixuan Zhang received the M.S. degree from Northeast Normal University, Changchun, China, in 2004, and the Ph.D degree from Northeastern University, Shenyang, China, in 2021. Since 2007, she is an instructor in Northeastern University at Qinhuangdao, Qinhuangdao, China. Her research interests include wireless communications, signal processing of communications, she is studying for a PhD in signal and information processing at Northeastern University. Her research interesting includes compressed sensing theory, signal processing of communications, and cognitive radio.

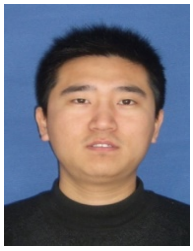

Zhenxing Sun received B.S. degree and M.S. degree from Northeast Petroleum University, Daqing, China,in 2003 and in 2011, respectively. He has been a doctoral student in Northeastern University, Shenyang, China, since 2015.Currently, he is an associate professor at Department of Electronics and Information Engineering Northeast Petroleum University at Qinhuangdao, China.